

NUREG/CR-3361

SAND83-1326

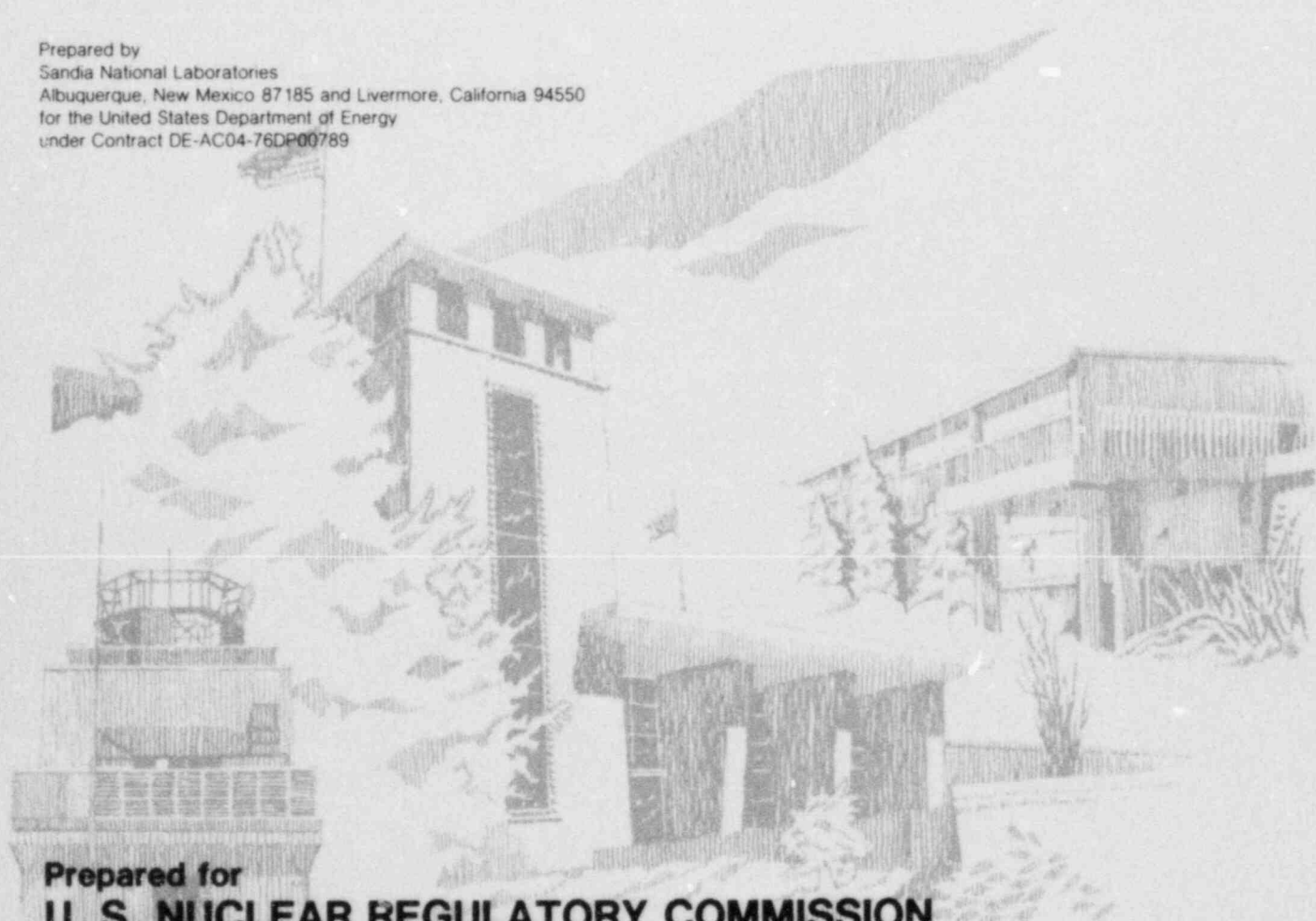
R3

Printed December 1984

# The Effect of Water Chemistry on the Rates of Hydrogen Generation From Galvanized Steel Corrosion at Post-LOCA Conditions

V. M. Loyola and J. E. Womelsduff

Prepared by  
Sandia National Laboratories  
Albuquerque, New Mexico 87185 and Livermore, California 94550  
for the United States Department of Energy  
under Contract DE-AC04-76DP00789



Prepared for  
**U. S. NUCLEAR REGULATORY COMMISSION**

SF 2900Q(B-81)

8502130366 850131

PDR NUREG

CR-3361 R

PDR

#### NOTICE

This report was prepared as an account of work sponsored by an agency of the United States Government. Neither the United States Government nor any agency thereof, or any of their employees, makes any warranty, expressed or implied, or assumes any legal liability or responsibility for any third party's use, or the results of such use, of any information, apparatus product or process disclosed in this report, or represents that its use by such third party would not infringe privately owned rights.

Available from  
GPO Sales Program  
Division of Technical Information and Document Control  
U.S. Nuclear Regulatory Commission  
Washington, D.C. 20555  
and  
National Technical Information Service  
Springfield, Virginia 22161

NUREG/CR-3361  
SAND83-1326  
R3

THE EFFECT OF WATER CHEMISTRY  
ON THE RATES OF HYDROGEN GENERATION FROM  
GALVANIZED STEEL CORROSION AT POST-LOCA CONDITIONS

V. M. Loyola and J. E. Womelsduff

December, 1984

Sandia National Laboratories  
Albuquerque, NM 87185  
Operated by  
Sandia Corporation  
for the  
U. S. Department of Energy

Prepared For  
Division of Accident Evaluation  
Containment Systems Research Branch  
Office of Nuclear Regulatory Research  
U. S. Nuclear Regulatory Commission  
NRC FIN No. A-1255

## ABSTRACT

The rates of hydrogen generation are measured for the corrosion of galvanized steel in three different light water cooled reactor (LWR) water chemistries. The results were obtained over a temperature range of 100° to 175°C and indicate that in a boiling water reactor (BWR) water chemistry, the reaction is faster than in those of two pressurized water reactors (PWR's).

A mechanism is proposed which would explain the observed results without requiring that the chemical additives come in direct contact with the corrodible unoxidized metal. Such a mechanism is required because electron microprobe analysis suggests that no chemical additives have diffused into the protective ZnO layer which forms on the unoxidized metal.

Arrhenius parameters are calculated for the three chemistries, but some questions are raised about whether those parameters are associated with a diffusion process or with the actual hydrogen producing reaction.

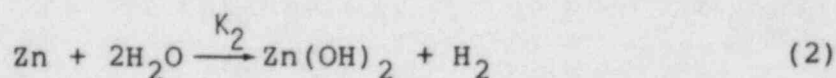
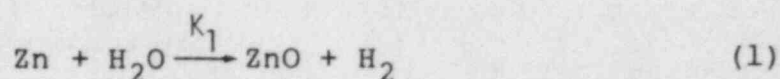
TABLE OF CONTENTS

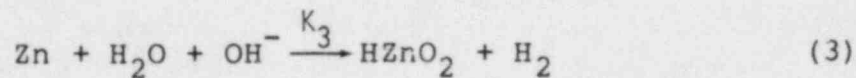
	<u>Page</u>
INTRODUCTION. . . . .	1
EXPERIMENTAL METHODS. . . . .	3
RESULTS AND DISCUSSION. . . . .	4
CONCLUSION. . . . .	9
REFERENCES. . . . .	11
TABLES. . . . .	12
FIGURES . . . . .	15

## INTRODUCTION

An inventory of nuclear power plants which were licensed for commercial operation in the United States as of December 31, 1979, indicates that 71 such plants exist.<sup>1</sup> Of that total, the large majority are light water cooled reactors (LWR's) with only one of another type, a high-temperature gas cooled reactor (HTGR), being licensed for commercial operation. Of the 70 licensed LWR's, 27 were classified as boiling water reactors (BWR's) and 43 as pressurized water reactors (PWR's). A further breakdown shows that 26 of the 27 BWR's have nuclear systems supplied by a single supplier; whereas, the PWR's nuclear systems are supplied by three different core manufacturers. In this report, the three different PWR nuclear systems will be referred to as PWR (I) for Westinghouse Corporation, PWR (II) for Combustion-Engineering, Inc., and PWR (III) for Babcock and Wilcox Co. The I, II, and III simply serve to indicate the different nuclear system suppliers and, therefore, different primary coolant chemistries. The 43 PWR's are equipped as follows: Approximately 60 percent are PWR (I), approximately 16 percent are PWR (II), and approximately 23 percent are PWR (III).

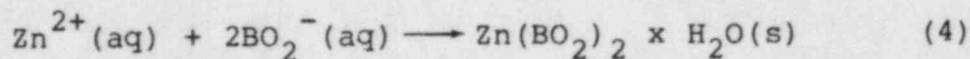
As indicated above, the primary coolant solutions and the emergency core cooling systems (ECCS) for each of these types of reactors are different, at least insofar as the chemistry of the coolant is concerned. Therefore, in the event of a loss-of-coolant-accident (LOCA) in a U. S. nuclear power plant, the interior surfaces of the containment building, which includes equipment for normal and emergency operation, walkways, gratings, and conduit could be exposed to the hot spilled coolant and containment spray solutions of any one of at least four different chemistries. According to design basis accident (DBA) analysis, the temperature within the containment building, and thus the temperature of the equipment, etc., could reach 150°C and might get higher depending on the severity of the accident. At the elevated temperatures which are predicted by DBA analysis, the corrosion of galvanized steel, from conduit, walkways, etc., according to Equations 1, 2, and 3, could become a concern.





The problems arising from these reactions are twofold. First, the hydrogen gas so produced can add to the hydrogen produced by other mechanisms (oxidation of the zirconium fuel cladding, radiolysis of water, etc.,) and thus contribute to the production of dangerously high levels of hydrogen within the containment building. If the quantity of combustible gas (i.e., hydrogen) in the containment reaches an ignitable level and does in fact ignite, the mixture can undergo either a rapid deflagration or build into a detonation. A detonation would be the worse of the two. In either case, a large quantity of heat is released, and a rapid pressure rise is produced. Such phenomena have a strong potential for complicating an accident because (1) the heat and pressure can damage or destroy equipment and instrumentation needed for accident mitigation, and (2) the pressure spike or possible shockwaves could exceed the building limits and cause venting of the containment to the atmosphere. Both conditions are extremely undesirable.

The second problem posed by the corrosion reactions concerns the nature of the other reaction products. Reactions 1 and 2 produce  $\text{ZnO}$  and  $\text{Zn(OH)}_2$ , respectively, both of which are very insoluble in aqueous media. The situation becomes more complex when the coolant solution is chemically modified by the addition of boric acid and/or tri-sodium phosphate as is done in PWR's. In PWR's, there is the additional concern of solids being formed via reactions of the type shown in Equations 4 and 5.



If such solid products formed, they would eventually settle to the bottom of the containment building sump where they could be picked up by the sump pumps and distributed throughout the ECCS. Such an occurrence could (1) cause fouling and failure of the sump pumps, (2) cause the solids to deposit in the ECCS heat exchangers, and/or (3) cause the solids to obstruct the nozzles of the containment spray system. Any of these conditions could result in diminished reactor cooling capacity and a worsening of an accident. It is important, therefore, to the design of

nuclear power plants that reactions of types 1, 2, and 3 be investigated.

The literature concerning hydrogen generation from zinc corrosion has been reviewed by Van Rooyen.<sup>3</sup> His review shows that there is a large scatter in the data available, and he concludes that in view of the potential hazards posed by these reactions, the data are few and that further investigation is needed. This report deals with reactions 1, 2, and 3 on galvanized steel and studies these reactions in three different aqueous media which are representative of the water chemistries of BWR, PWR (I), and PWR (II) reactors.

#### EXPERIMENTAL METHOD

The corrosion of galvanized steel was studied using aqueous solutions of three different chemical compositions. These solutions are referred to in this paper as BWR, PWR (I), and PWR (II) and have the following composition:

BWR: Demineralized water;  $5.3 \leq \text{pH} \leq 8.6$  at ambient.

PWR (I): 0.18 molar  $\text{H}_3\text{BO}_3$  (2000 ppm B);  $8.5 \leq \text{pH} \leq 9.0$  at ambient, the pH was adjusted with NaOH.

PWR (II): 0.25 molar  $\text{H}_3\text{BO}_3$  (2680 ppm B), 1.6 mmolar  $\text{H}_2\text{NNH}_2$  (50 ppm); 3.1 mmolar  $\text{Na}_3\text{PO}_4 \cdot 12\text{H}_2\text{O}$  (1170 ppm);  $7 \leq \text{pH} \leq 7.7$  at ambient.

All solutions were prepared using demineralized water having a resistivity  $\geq 10^7$  ohm/cm. All chemicals were of reagent grade quality, or better. Measurements of pH were made at ambient conditions with standard buffers as references.

The galvanized steel samples were prepared from ASTM A36 steel plate cut to dimensions of 5.08 cm x 10.16 cm x 0.305 cm with corners rounded to a radius of 0.318 cm. The samples were coated with zinc by the hot-dip process according to ANSI/ASTM A-123-78 standards. The coated samples were individually washed and degreased, wrapped in soft paper, and stored at ambient conditions in a desiccator until used.

Corrosion tests were carried out in a specially designed, stainless steel vessel, which has been described previously,<sup>4</sup> and the samples were completely immersed in the test solution during the test. Each test was of 24-hour duration, and the rate of hydrogen generation was measured by periodically sampling the reactor atmosphere and performing a gas



chromatographic analysis for hydrogen concentration. The reactor atmosphere was sampled by a gas chromatograph programmed to manipulate a series of sampling valves. The gas chromatograph was calibrated between tests at each test temperature by charging the reactor vessel with known quantities of ultra-high purity H<sub>2</sub> gas and sampling the atmosphere in the same manner as during a test. For the calibration procedure, there was no sample in place, and demineralized water was used to reproduce the humid atmosphere within the vessel. After completion of a test, the reactor vessel was allowed to cool to near ambient conditions and disassembled. The test solution was collected in a glass beaker and examined for the presence of suspended solids. If solids were present in sufficient quantity, the solution was filtered, and the solids collected. The test vessel was then cleaned and dried and prepared for the next test. This procedure was followed for all tests as well as for calibrations.

Analysis of reaction products which adhered to the galvanized steel samples were obtained using scanning electron microscopy (SEM), electron microprobe analysis (EMA), and x-ray photoelectron spectroscopy (XPS). Energy dispersive EMA elemental maps were obtained for Fe, Zn, O, B, P, S, and Pb using a 15 kV electron beam of 20-85 na current. Reaction products which cracked and detached from the substrate were analyzed by XPS for unoxidized Zn.

## RESULTS AND DISCUSSION

All test solutions were collected and examined for the presence of suspended solids. The solutions were usually very clean and clear with particulate matter occurring only in a few cases. When material was present and the solution filtered, only very small quantities of matter were collected and usually contained small fibers. The fibers are believed to have originated from either the soft paper in which the samples were wrapped for storage or from the glass fiber insulation used around the reactor vessel. Solid reaction products generally tend to remain adhered to the steel substrate. Except in the case where samples were corroded at high temperature (~175°C), the adhered products were very tenacious and could not be readily removed. In the case of samples corroded at high temperature, the reaction products were very brittle at the edges of the sample and broke away from the sample during handling. In the areas where the product layer failed, the product usually came away completely and exposed the steel substrate (see Figures 1 and 2). The detachment and fracturing of the product layer are indicative of extensive reaction

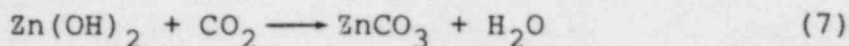
extending to the steel substrate and, presumably, total consumption of the galvanized coating. XPS analysis shows these products to be ZnO with no unoxidized Zn present. The presence of the iron (Figure 1c) throughout the product is probably due to alloying during the hot-dipping process, and not to extensive diffusion of reacted steel.

Except for the case where the reaction is so extensive that the products crack and fall away from the substrate, it is difficult to assess the extent of reaction from the electron microprobe analysis data. Molecular oxygen tends to adsorb on surfaces, especially metals and metal oxides. In our case, it is difficult to separate the adsorbed oxygen signal from the product oxygen signal, i.e., signal from oxides of Zn and Fe. Figure 3a shows the oxygen adsorbed onto the surface of an uncorroded sample which has been ground and polished for analysis. The problem of adsorbed oxygen is not trivial because the grinding and polishing must be done away from the analytical instrument and the samples transferred into it afterwards. Grinding and polishing all samples in an argon atmosphere did not yield different results. Figure 3b is a scanning electron microscope photomicrograph of the unreacted sample, and it shows the absence of cracks in the galvanized coating. There are some small voids present which were probably caused by bubbles during the galvanizing process. Figure 4 is similar photomicrographs of samples corroded at high temperature ( $\sim 175^{\circ}\text{C}$ ) in the three chemistries of interest. All show the cracking and large voids suggesting extensive reaction.

Figure 5a is an SEM photomicrograph of a different section of the sample shown in Figure 4c. It also shows cracking and voids. Figure 5b is an energy dispersive electron photomicrograph for phosphorus of that same section. It shows that the phosphate of the PWR (II) solution has deposited onto the surface of the reaction product, but that none have diffused into or penetrated the product layer. Similar photomicrographs for boron using samples corroded in both PWR (I) and PWR (II) solutions fail to show any diffusion of borates. Within the limits of detection of the electron microprobe technique, there is no boron either in the product layer or on the product surface. The absence of both phosphates and borates in the product and the absence of suspended solids in solution suggest that reactions 4 and 5 are not of major importance in these systems. The important reactions then are probably reactions 1, 2, and 3, so far as hydrogen generation is concerned, and probably include reactions such as reaction 6 in the overall corrosion process.



There is no evidence for the occurrence of reaction 7 which would tend to passivate the surface to further reaction.



This is not surprising because studies have shown that at temperatures well below those of these studies, zinc hydroxide will convert to zinc oxide<sup>5,6,7</sup> and, thus, should inhibit carbonate formation.

Figures 5a, b, and c are an SEM photomicrograph, an electron microprobe map for Fe, and an electron microprobe map for Zn, respectively, of a sample corroded at 154°C in demineralized water. Figure 6 shows that in some cases, there is pitting of the surface layer and probable galvanic corrosion. Establishment of micro-galvanic cells at pitted areas means that the corrosion mechanism over the entire coupon surface is non-uniform and quite complex. Because of the possible pitting and very large extent of reaction associated with the tests at high temperature, we feel that the change in rate of hydrogen production which is evident in Figures 7 and 8 at 175°C is probably due to both a depletion of reactive material as well as to a nonhomogeneous surface. If a nonhomogeneous surface is reacting, then it is meaningless to report rate constants in terms of  $\text{SCM/m}^2\text{-hr}$  because the surface area is no longer known. For this reason, only the initial rates of hydrogen production are reported at high temperature, and no attempt is made to calculate a rate constant for the slower part of the reaction. Typical  $\text{H}_2$  concentration versus time plots for the three chemistries of interest are shown in Figures 7, 8, and 9, and the measured rate constants are given in Tables 1, 2, and 3.

The electron microprobe analysis of the reaction products, which was discussed above, raises some interesting questions about what processes are actually being measured in these and other studies of this nature. The absence of borates and phosphates in the reaction product matrix suggests that these chemicals are being excluded from the reactive regions which are rich in zinc/zinc-iron alloy, and that the pertinent reactions are of the nature of reactions 1, 2, 3, and 6. However, if this were the case, then one would expect that at the reactive

surface the reaction mechanisms and, therefore, the rates would be the same for all three chemistries. Tables 1-3 and Figures 7-9 clearly show that such is not the case. A reasonable explanation for the chemical dependence of the rates, then, is that the chemical additives are changing the chemical nature of and the rate at which the reactive species reach the unoxidized surface. It has been suggested previously that corrosion is caused by differences at the metal surface, differences in oxygen content, salinity, pH, etc., between the metal surface, and the environment. We would like to expand on this and suggest that differences in corrosion or corrosion rates can also be caused by differences at the surface of the product layer. Figure 5b clearly shows that chemical additives can deposit on the product layer and could then induce chemical changes in the corrosive medium which is diffusing to the reactive surface. The same is true even in cases where no deposition is observed, i.e., the borated solutions, because hydrogen bonding and dipolar interactions between the surface and chemical species in the solution can lead to significant chemical changes at the surface of the product layer. The fact that the demineralized water corrodes the galvanized steel more efficiently than the chemically modified solutions was unexpected; however, when one considers that the demineralized water has no buffering ability and that there are no additives and/or surface deposits to hinder diffusion of the  $H_2O$ ,  $OH^-$ ,  $O_2$ , etc., to the reactive material, the same observation should not be surprising. It is not clear, then, that the rates which are measured in this type of study are strictly the rates of reactions 1, 2, and 3, and may instead be highly influenced by the rates of diffusion of steam, oxygen, hydroxyl ion, etc., through the product layer. We suspect, then, that the induction periods seen in Figures 7-9 may be due to an equilibration period between the hot-dry initial oxide layer, which has been protected during heating by the sample holder, and the hot corrosion medium, prior to the onset of reactions 1-3. We, nevertheless, will report our data as rate constants for  $H_2$  generation and will treat these rates as if due to a relatively simple overall hydrogen generating reaction. We have calculated our rate constants from the data subsequent to the induction period and, thus, obtained the maximum rates of hydrogen production. Reporting our data in this manner will allow us to use standard kinetic equations (Equations 8 and 9) to calculate activation parameters for the overall process.

$$k = A \exp(-E_a/RT) \quad (8)$$

$$\ln k = \ln A - E_a/RT \quad (9)$$

where

A = A pre-exponential factor having units of SCM/m<sup>2</sup>-hr

E<sub>a</sub> = Activation energy for the H<sub>2</sub> generating process in cal/mole

R = Universal gas constant in units of cal/deg-mole

T = Absolute temperature

Tables 1, 2, and 3 contain the data which were collected for these systems, and comparison to literature<sup>9,10</sup> values show that our values tend to be higher, often by as much as an order of magnitude. Figures 10, 11, and 12 are our data plotted according to Equation 9 and yield activation energies which are about 10 kcal/mole higher than the average of 14.5 kcal/mole calculated by Van Rooyen from the work of several authors. These differences can arise from several reasons:

- (1) Test materials: Much of the available data were collected using zinc-rich paint primers, as opposed to galvanized steel.
- (2) Test methods: Most of those tests were conducted by immersing the samples in the test solution and then heating to temperature, as opposed to heating everything to temperature prior to sample exposure.
- (3) Test duration: Those tests were carried out using integral tests, i.e., a sample was corroded for 24 hours, 48 hours, 72 hours, and sometimes longer periods prior to measurement of H<sub>2</sub> generation, and the results integrated over the entire time period.

Differences in materials, especially in going from a flat surface area to a fine powder surface as found in zinc-rich primers, can result in huge differences in reactivity. One would expect that the higher surface area of the zinc powder in the primers would result in higher apparent reaction rates. The literature data do not support this since reported rates are typically lower than our values. Our own data, however, do support that expectation and indicate that test duration may be

partially responsible for the low literature values. Our data with zinc primers<sup>11</sup> indicate that the initial rate of hydrogen evolution from primers is very high, and the reaction over in 4-5 hours, continuing to age the samples for as long as 48 or 72 hours prior to sampling would result in calculated rate constants considerably lower than the initial rates would indicate. Test methods could also account for some of the disagreement within the literature as well as with our data. Immersion of the test samples prior to heating to temperature will result in continuously changing reaction rates due to temperature induced changes in the nature of the coating. The literature<sup>5,6,7</sup> contains much evidence to support changes of this nature.

### CONCLUSION

Our studies of hydrogen evolution from hot water corrosion of galvanized steel indicate that the demineralized water solutions which are typical of BWR reactors are more efficient hydrogen producers than the chemically modified solutions of the two PWR type reactors considered. The rates of hydrogen evolution were higher and the activation energies lower, over the temperature range studied, for the BWR solution than for either of the PWR solutions. Electron microprobe analysis of sectioned samples show that the reaction products, which are tightly adhered to the surface of the steel substrate, are primarily oxides of iron and zinc and that the boric acid and sodium phosphate additives of the PWR (I) and (II) solutions do not penetrate the oxide layer. In the case of the phosphate, it is seen to deposit on the water side of the oxide layer, but not to progress any further. It appears that the chemical additives of the PWR (I) and (II) solutions affect the rates of H<sub>2</sub> evolution by changing the chemistry of the corrosive medium at the surface of the oxide layer. Changing factors such as pH, salinity (i.e., conductivity), oxygen content, and rates of diffusion at the surface could account for differences in rate. These observations suggest that this type of study does not actually measure the elementary processes of Equations 1-3, but instead measures the complex processes of diffusion through the oxide layer and how that is affected by changes in temperature and chemistry.

Our data are typically higher than most of the data found in the literature. We attribute this to differences in temperature ranges studied and methodology of the experimentation, as well as to differences in chemistry. Much of the testing done to date has been carried out over temperature ranges considerably different than that of our work. Several studies have shown

that the nature of the oxide layer, i.e., density, tenacity, and hardness, as well as chemistry, undergoes definite changes over certain temperature ranges<sup>5,6,7,12</sup> and that these factors do influence rates. Our own previous work<sup>4</sup> indicates that there is nonlinear behavior in plots such as those in Figures 10, 11, and 12 when the temperature range is too broad. The experimental methodology employed in many previous studies involved immersing the test samples in the test solutions prior to raising the temperature of the solution to the required value. Our procedure was to keep the sample isolated until the entire test apparatus, including the sample, was at the required temperature. Also, most of the previous studies allowed the reaction to proceed for a predetermined period of time, usually for several hours prior to sampling the product atmosphere for H<sub>2</sub>. Our approach was to conduct the tests for 24-hour periods with frequent sampling throughout that time. Much of the data collected to date has been collected using zinc-rich paint primers as test samples. We have tested both galvanized steel and primers. Our tests indicate that at high temperature, and especially for the primers, the initial rate of H<sub>2</sub> evolution is quite high and that evolution ceases after a few hours. Tests conducted for 24, 72, or 100 hours and then extrapolated to zero time would by necessity result in lower rates than would a measurement of the initial rate. We feel that our tests are more indicative of what one can expect immediately following a large-scale LOCA.

The production of solid materials from post-LOCA reactions is of great concern to reactor safety engineers, as it should be, because of the potential of such materials for fouling ECCS apparatus. One source of such solid material is the corrosion of zinc to form oxides, hydroxides, and borates and phosphates as shown in Equations 4 and 5. Our studies show that within a temperature range of 100° to 175° C and for relatively short periods of exposure (24 hours), the production of such materials is not a problem. The oxide products formed are insoluble and adhere very tenaciously to the steel substrate and inhibit diffusion of borates/phosphates to the zinc surface. One should bear in mind, however, that these tests were carried out for 24 hours and the samples removed very shortly thereafter. Thus, we have no information as to the behavior of these materials either after long periods of standing in the reactor solutions or after a hydrogen burn.

We are, as indicated earlier in the text of this report, continuing similar studies involving zinc-rich primers and primers with topcoats. We expect to complete those studies in the near future.

## REFERENCES

1. Nuclear News, February, 1980, p. 67.
2. K. K. Niyogi, R. R. Lunt, and J. S. MacKenzie, "Corrosion of Aluminum and Zinc in Containment Following a LOCA and Potential for Precipitation of Corrosion Products in the Sumps," United Engineers and Constructors, Inc., presented at the Workshop on the Impact of Hydrogen on Water Reactor Safety, Albuquerque, New Mexico, October, 1982.
3. D. Van Rooyen, "Hydrogen Release Rates from Corrosion of Zinc and Aluminum," BNL-NUREG-24532, Brookhaven National Laboratory (1978).
4. V. M. Loyola and J. E. Womelsduff, "The Relative Importance of Temperature, pH, and Boric Acid Concentration of Rates of H<sub>2</sub> Production from Galvanized Steel Corrosion," SAND83-1179, NUREG/CR-2812, Sandia National Laboratories (1983).
5. G. L. Cox, "Effect of Temperature on the Corrosion of Zinc," Industrial and Engineering Chemistry, Vol. 23, No. 8 (1931), pp. 902-904.
6. John F. Montle, "Analysis of Problems in Protective Coatings Applications," International Corrosion Forum Devoted Exclusively to the Protection and Performance of Materials, San Francisco, California, March, 1977, Paper No. 2.
7. L. Shinozawa, "Corrosion of Zinc," Thesis, Case Institute of Technology (1950).
8. Hugh P. Goddard, "Corrosion of Metals by Waters," Materials Performance, NACE, May (1979), pp. 21-27.
9. L. E. S. Smith, R. D. Lane, and W. Alexander Van Hook, "Experimental Modeling of Hydrogen Evolution Rates from Surfaces with Exposed Zinc Metal or Zinc Primer Coating in Contact with Containment Sprays in PWR Nuclear Power Plants," Nuclear Technology, Vol. 53 (1981), pp. 388-391.
10. H. E. Zittel, "Post-Accident Hydrogen Generation from Protective Coatings in Power Reactors," Nuclear Technology, Vol. 17 (1973), pp. 143-146.
11. V. M. Loyola, J. E. Womelsduff, Results to be published, Sandia National Laboratories.



TABLE 1

Rate Constants for H<sub>2</sub> Evolution from  
Galvanized Steel in BWR Test Solution

<u>Temp., °C</u>	<u>pH</u>	<u>Rate Constant SCM/m<sup>2</sup>-hr</u>	<u>Weight Gain gram/sample</u>
100.9 ± 1.1	7.46	(1.11 ± .04) X10 <sup>-4</sup>	0.0354
131.6 ± 1.1	6.59	(1.11 ± .07) X10 <sup>-3</sup>	0.1964
131.8 ± 1.1	6.33	(1.29 ± .08) X10 <sup>-3</sup>	0.2183
151.1 ± 1.3	7.30	(5.27 ± .16) X10 <sup>-3</sup>	0.8275
152.9 ± 1.3	7.34	(3.99 ± .16) X10 <sup>-3</sup>	0.5015
176.0 ± 1.1	6.15	(1.11 ± .05) X10 <sup>-2</sup>	1.5181
175.2 ± 1.1	5.97	(1.12 ± .05) X10 <sup>-2</sup>	1.3138

TABLE 2

Rate Constants for H<sub>2</sub> Evolution from  
Galvanized Steel in PWR(I) Test Solution

<u>Temp., °C</u>	<u>pH</u>	<u>Rate Constant</u> <u>SCM/m<sup>2</sup>-hr</u>	<u>Weight Gain</u> <u>gram/sample</u>
100.5 ± 1.3	8.96	(2.90 ± .33) X10 <sup>-5</sup> <sup>a,b</sup>	0.0055
132.3 ± 0.9	9.02	(2.48 ± .27) X10 <sup>-4</sup>	0.0332
132.1 ± 1.1	8.97	(2.17 ± .18) X10 <sup>-4</sup> <sup>c</sup>	0.0379
152.2 ± 1.3	8.98	(3.86 ± .30) X10 <sup>-3</sup>	0.5070
153.1 ± 1.3	8.96	(2.81 ± .20) X10 <sup>-3</sup>	0.3327
175.0 ± 1.3	8.97	(7.61 ± .63) X10 <sup>-3</sup>	0.9575
175.2 ± 1.1	8.98	(8.49 ± .38) X10 <sup>-3</sup>	1.0195

a) Ref. 9; Zinc metal @ 99°C, pH 9.8, 2270 ppm B, rate constant =  $6.0 \times 10^{-6}$  SCM/m<sup>2</sup>-hr.

b) Ref. 9; Zinc metal @ 106°C, pH 9.8, 2270 ppm B, rate constant =  $7.2 \times 10^{-6}$  SCM/m<sup>2</sup>-hr.

c) Ref. 10; Galvanized steel @ 130°C, pH 9.3, 3000 ppm B, rate constant =  $1.01 \times 10^{-3}$  SCM/m<sup>2</sup>-hr.

TABLE 3

Rate Constants for H<sub>2</sub> Evolution from  
Galvanized Steel in PWR(II) Test Solution

<u>Temp., °C</u>	<u>pH</u>	<u>Rate Constant SCM/m<sup>2</sup>-hr</u>	<u>Weight Gain gram/sample</u>
101.3 ± 1.3	6.91	(2.49 ± .34) X10 <sup>-5</sup> <sup>a</sup>	0.0195
131.0 ± 1.3	6.90	(2.16 ± .13) X10 <sup>-4</sup>	0.0452
131.6 ± 1.1	6.90	(2.41 ± .05) X10 <sup>-4</sup>	0.0528
152.9 ± 1.3	6.90	(2.43 ± .13) X10 <sup>-3</sup>	0.2982
152.8 ± 1.1	6.90	(2.04 ± .19) X10 <sup>-3</sup> <sup>b</sup>	0.2467
175.0 ± 1.1	6.87	(4.30 ± .13) X10 <sup>-3</sup>	0.8271
175.6 ± 1.1	6.95	(3.91 ± .19) X10 <sup>-3</sup>	0.6595

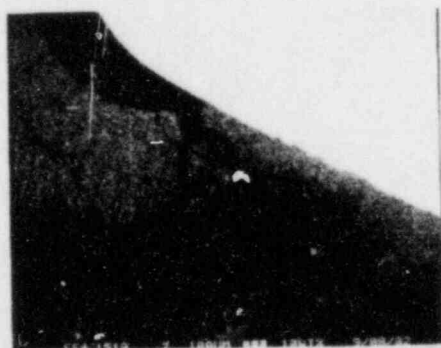
- a) Ref. 9; Galvanized steel @ 106°C, 3800 ppm B, 50 ppm H<sub>2</sub>NNH<sub>2</sub>, TSP to give pH 7.5, rate constant = 6.7 X 10<sup>-5</sup> SCM/m<sup>2</sup>-hr.
- b) Ref. 9; Zinc metal @ 151°C, 3800 ppm B, 50 ppm H<sub>2</sub>NNH<sub>2</sub>, TSP to give pH 7.5, rate constant = 2.7 X 10<sup>-4</sup> SCM/m<sup>2</sup>-hr.



a



b



c



d

FIGURE 1: SEM and Electron Microprobe Photographs of Cracked and Detached Coating of BWR Test Sample.

a) SEM Photograph Shows Failure Of Coating At Edges Of Sample and Indicates Extensive Reaction.

b,c,d) Electron Microprobe Indicates Composition Of Product To Be Zn/Fe Oxides and Shows Alloying Effects Of Galvanizing Process. Photographs b, c, and d Are For Zn, Fe, and O, Respectively.

The light areas indicate the presence of the element of interest, dark areas indicate an absence of that element. For example, b and d show that Zn and O are both present in the same regions, suggesting an oxide of zinc.



a



b

FIGURE 2: SEM Photographs of Detached Corrosion Product From 175°C BWR Test. Electron Microprobe Indicates Only Oxides of Fe and Zn.

a) 100X

b) 200X



a



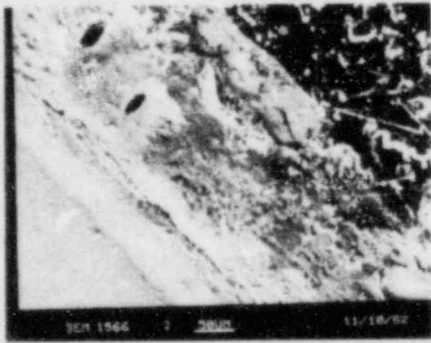
b

FIGURE 3: Uncorroded Galvanized Sample.

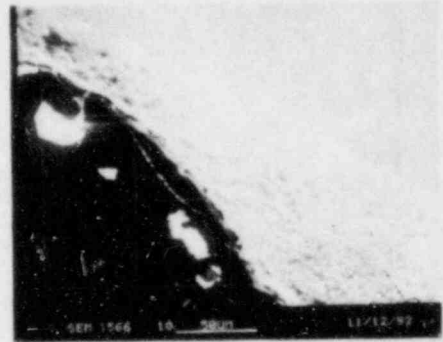
a) SEM Photograph, 400X, Shows No Cracking and Only Very Small Voids.

b) Electron Microprobe Map Of Surface Showing Oxide Layer On Polished Metal.

- a) BWR, 200X
- b) PWR(I), 400X
- c) PWR(II), 400X



a

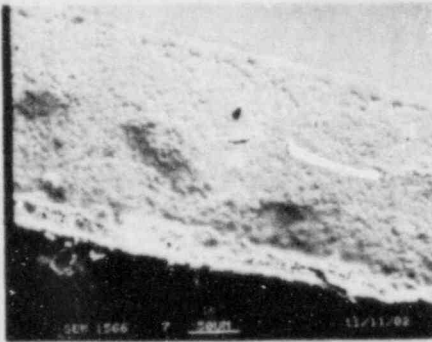


b

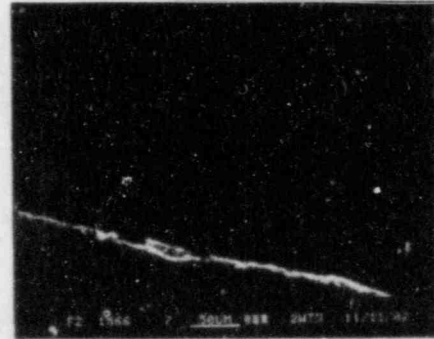


c

FIGURE 4: SEM Photographs of Samples Corroded at 175°C. All Samples Show Extensive Cracking and Voids.



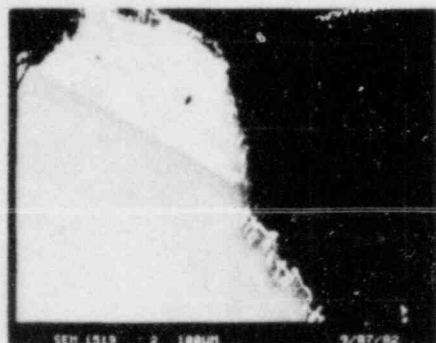
a



b

FIGURE 5: SEM and Electron Microprobe Photographs of Sample Corroded at 175°C in PWR(II) Solution.

- a) SEM Shows Cracking, Voids, and Deposits On Water Side Of Surface 200X.
- b) Electron Microprobe Analysis Of Same Surface Shows Deposits To Contain Phosphorous.



a



b



c

FIGURE 6: SEM and Electron Microprobe Photographs of Sample Corroded at 152°C in BWR Solution.

- a) SEM Shows Corrosion Into Steel Substrate Suggesting Action Of Galvanic Microcell, 200X.
- b,c) Electron Microprobe Maps Of Fe and Zn, Respectively, Showing Presence Of Zn In Pitted Area.



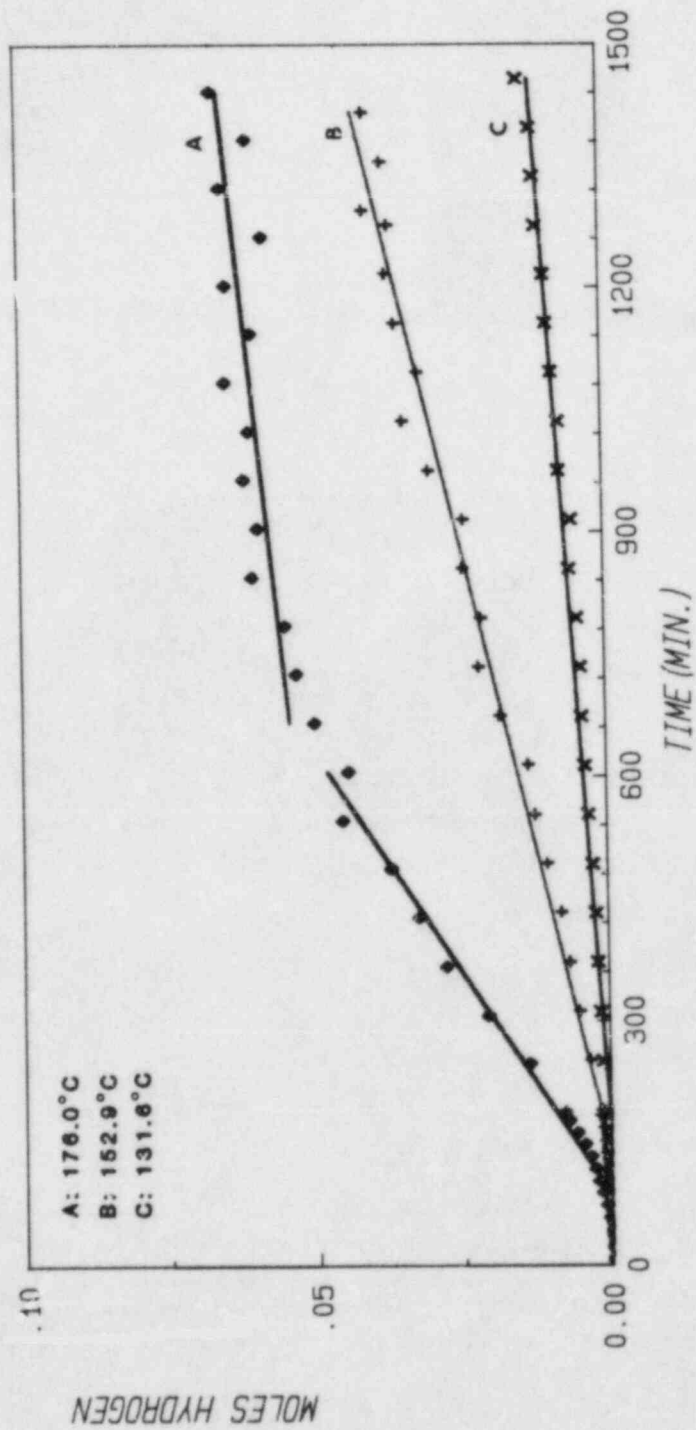


FIGURE 7: Corrosion of Galvanized Steel by BWR Solution.

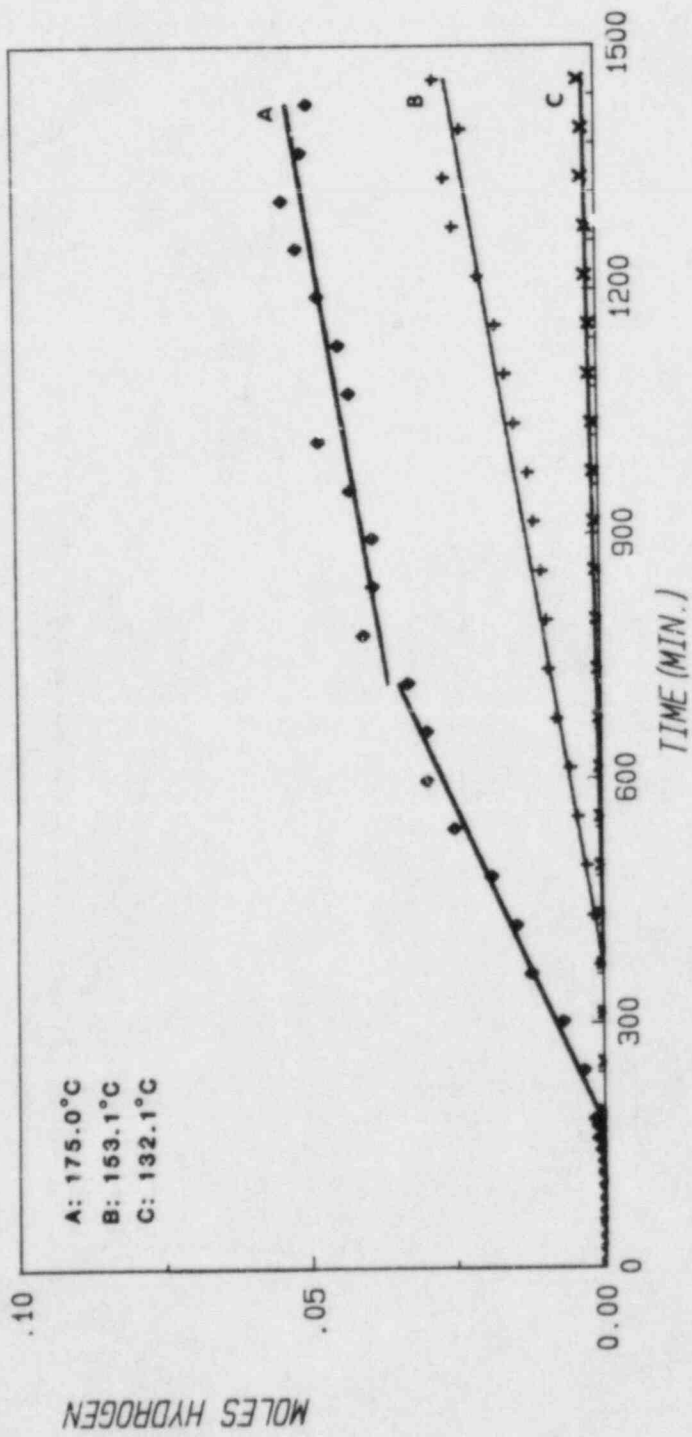


FIGURE 8: Corrosion of Galvanized Steel by PWR(1) Solution.

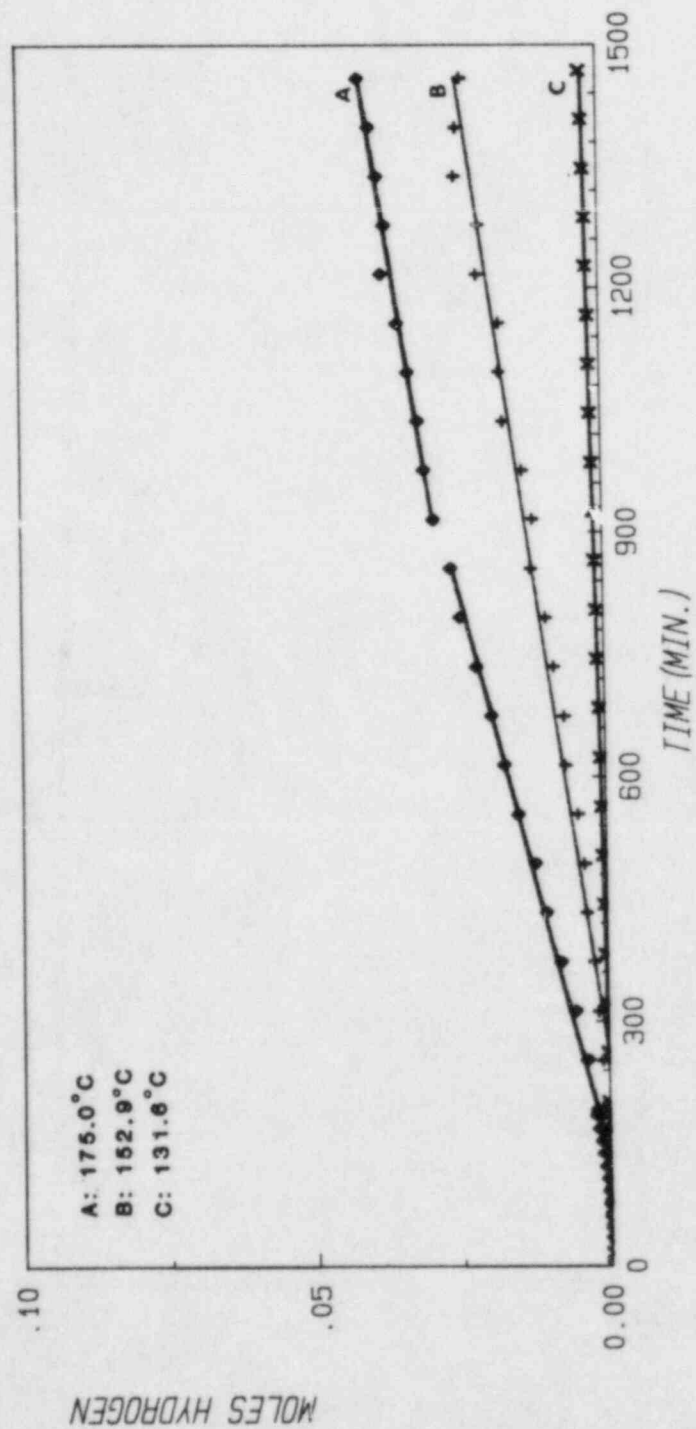


FIGURE 9: Corrosion of Galvanized Steel by PWR(II) Solution.

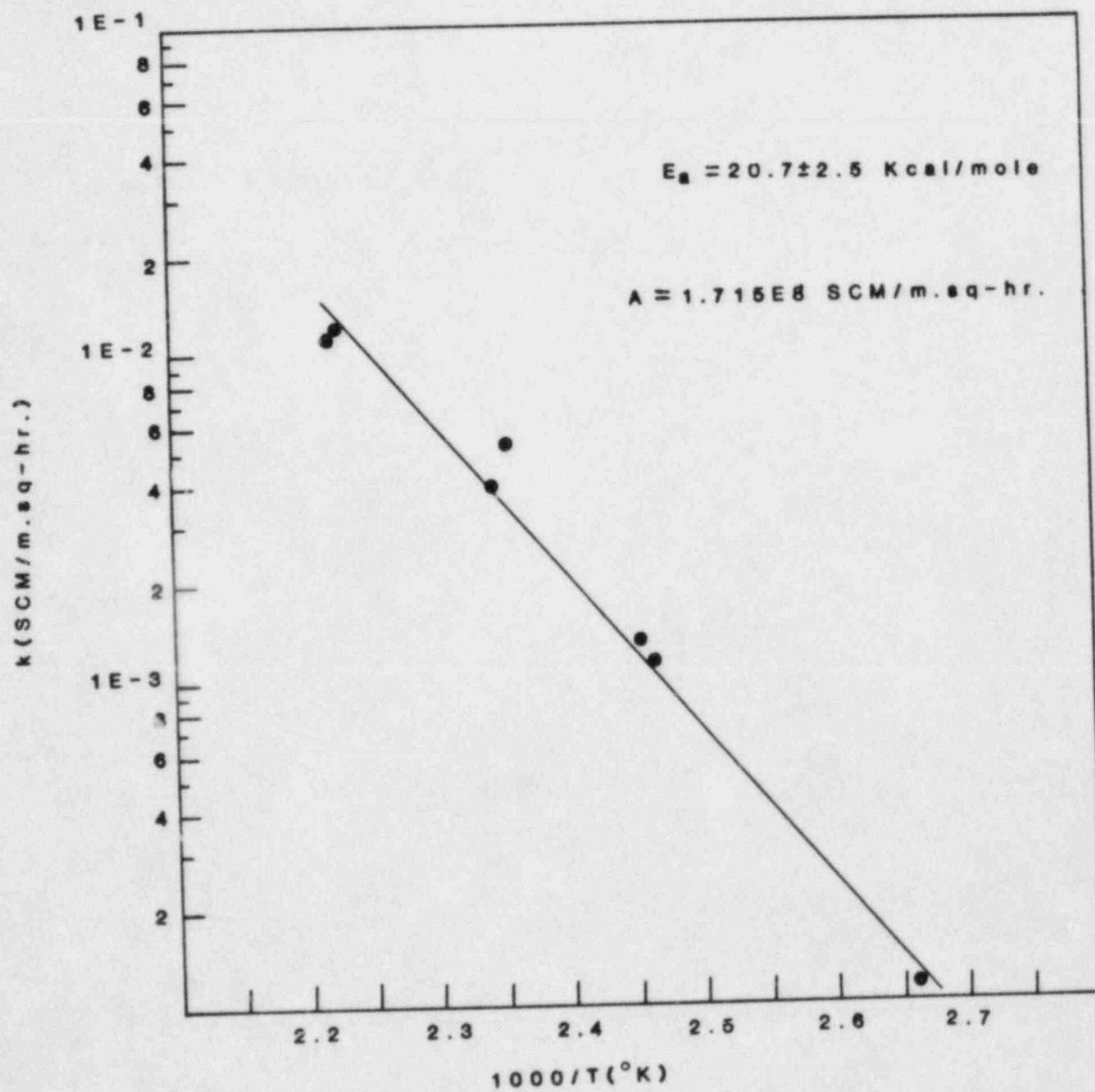


FIGURE 10: Arrhenius Plot For BWR Solution

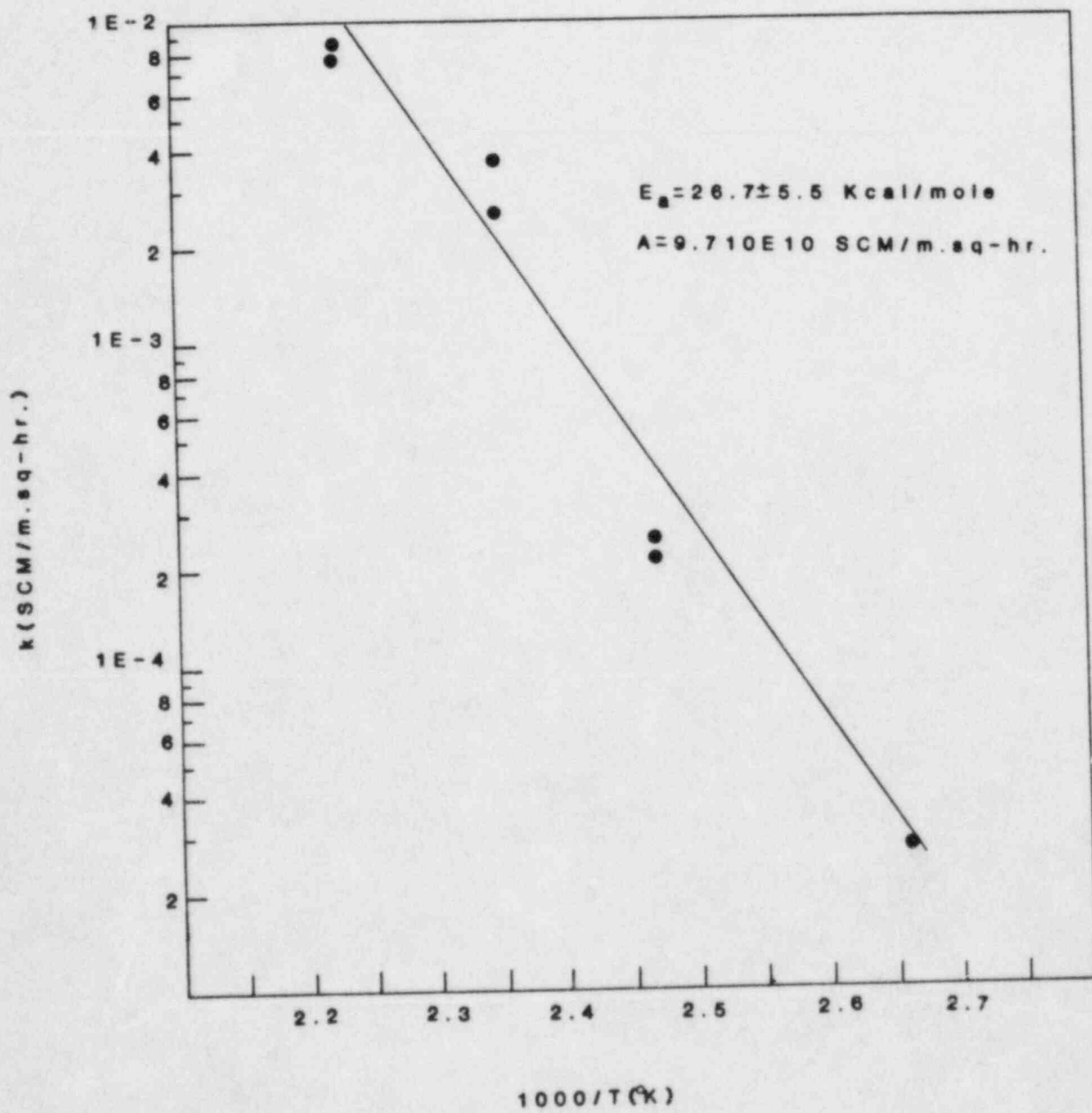


FIGURE 11: Arrhenius Plot For PWR(I) Solution.

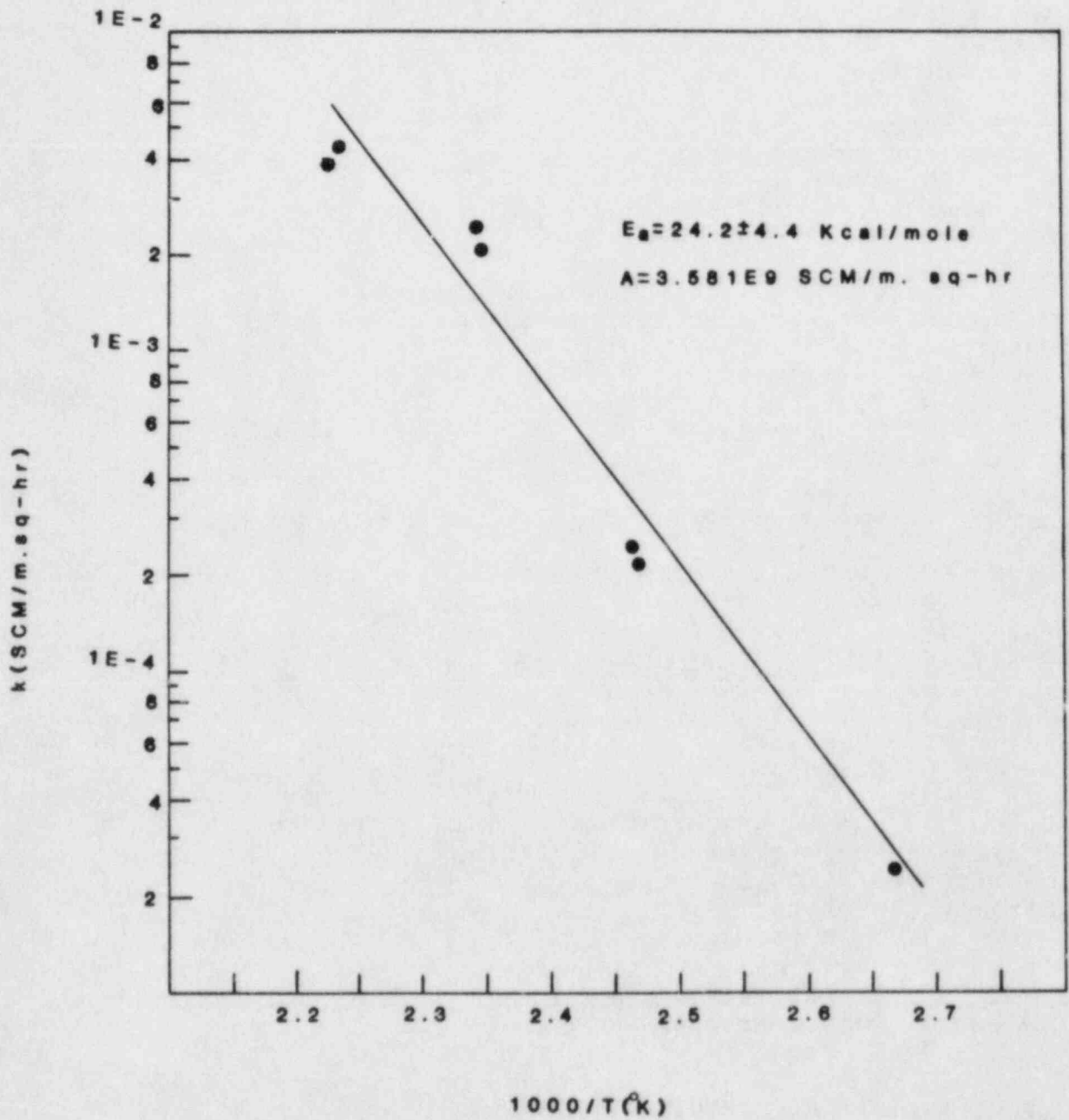


FIGURE 12: Arrhenius Plot For PWR(II) Solution.

Distribution:

Division of Technical Information  
and Document Control  
NRC Distribution Contractor  
U.S. Nuclear Regulatory Commission  
15700 Crabbs Branch Way  
Rockville, MD 20850  
275 copies for R3

U. S. Bureau of Mines  
Pittsburgh Research Center  
P. O. Box 18070  
Pittsburgh, PA 15236  
Attn: M. Hertzberg

U. S. Nuclear Regulatory Commission (6)  
Office of Nuclear Regulatory Research  
Washington, DC 20555  
Attn: G. A. Arlotto  
R. T. Curtis  
J. T. Larkins  
L. C. Shao  
K. G. Steyer  
P. Worthington

U. S. Nuclear Regulatory Commission (5)  
Office of Nuclear Regulatory Research  
Washington, DC 20555  
Attn: B. S. Burson  
M. Silberberg  
J. L. Telford  
T. J. Walker  
R. W. Wright

U. S. Nuclear Regulatory Commission (6)  
Office of Nuclear Reactor Regulation  
Washington, DC 20555  
Attn: J. K. Long  
J. F. Meyer  
R. Palla  
K. I. Parczewski  
G. Quittschreiber  
D. D. Yue

U. S. Nuclear Regulatory Commission (6)  
Office of Nuclear Reactor Regulation  
Washington, DC 20555  
Attn: V. Benaroya  
W. R. Butler  
G. W. Knighton  
T. M. Su  
Z. Rosztoczy  
C. G. Tinkler

U. S. Department of Energy  
Operational Safety Division  
Albuquerque Operations Office  
P.O. Box 5400  
Albuquerque, NM 87185  
Attn: J. R. Roeder, Director  
Dr. M. Peehs

Acurex Corporation  
485 Clyde Avenue  
Mountain View, CA 94042

Applied Sciences Association, Inc.  
P. O. Box 2687  
Palos Verdes Pen., CA 90274  
Attn: D. Swanson

Argonne National Laboratory  
9700 South Cass Avenue  
Argonne, IL 60439  
Attn: H. M. Chung

Astron  
2028 Old Middlefield Way  
Mountainview, CA 94043  
Attn: Ray Torok

Battelle Columbus Laboratory  
505 King Avenue  
Columbus, OH 43201  
Attn: P. Cybulskis  
R. Denning

(2)

Bechtel Power Corporation  
P. O. Box 3965  
San Francisco, CA 94119  
Attn: R. Tosetti

Bechtel Power Corporation  
15740 Shady Grove Road  
Gaithersburg, MD 20877  
Attn: D. Ashton

Brookhaven National Laboratory  
Upton, NY 11973  
Attn: R. A. Bari  
T. Pratt

(2)



Duke Power Co.  
P. O. Box 33189  
Charlotte, NC 28242  
Attn: F. G. Hudson (2)  
A. L. Sudduth

EG&G Idaho  
Willow Creek Building, W-3  
P. O. Box 1625  
Idaho Falls, ID 83415  
Attn: Server Sadik

Electric Power Research Institute  
3112 Hillview Avenue  
Palo Alto, CA 94303  
Attn: J. J. Haugh (3)  
K. A. Nilsson  
G. Thomas

Factory Mutual Research Corporation  
P. O. Box 688  
Norwood, MA 02062  
Attn: R. Zalosh

Fauske & Associates  
627 Executive Drive  
Willowbrook, IL 60521  
Attn: R. Henry

General Electric Co.  
175 Curtner Avenue  
Mail Code N 1C157  
San Jose, CA 95125  
Attn: K. W. Holtzclaw

General Physics Corporation  
1000 Century Plaza  
Columbia, MD 21044  
Attn: Chester Kupiec

Los Alamos National Laboratory  
P. O. Box 1663  
Los Alamos, NM 87545  
Attn: H. S. Cullingford (4)  
R. Gido  
G. Schott  
J. Travis

University of Michigan  
Department of Aerospace Engineering  
Ann Arbor, MI 47109  
Attn: Martin Sichel

Mississippi Power & Light  
P. O. Box 1640  
Jackson, MS 39205  
Attn: S. H. Hobbs

Northwestern University  
Chemical Engineering Department  
Evanston, IL 60201  
Attn: S. G. Bankoff

NUS Corporation  
4 Research Place  
Rockville, MD 20850  
Attn: R. Sherry

Offshore Power System (2)  
8000 Arlington Expressway  
Box 8000  
Jacksonville, FL 32211  
Attn: G. M. Fuls  
D. H. Walker

Power Authority State of NY  
10 Columbus Circle  
New York, NY 10019  
Attn: R. E. Deem (2)  
S. S. Iyer

Purdue University  
School of Nuclear Engineering  
West Lafayette, IN 47907  
Attn: T. G. Theofanous

Sandia National Laboratories  
Directorate 6400  
P. O. Box 5800  
Albuquerque, NM 87185  
Attn: R. Cochrell (20)

Sandia National Laboratories  
Organization 6427  
P. O. Box 5800  
Albuquerque, NM 87185  
Attn: G. Shaw (20)

Dr. Roger Strehlow  
505 South Pine Street  
Champaign, IL 61820

TVA  
400 Commerce  
W9C157-CD  
Knoxville, TN 37902  
Attn: Wang Lau

Thompson Associates  
639 Massachusetts Avenue  
Third Floor  
Cambridge, MA 02139  
Attn: Timothy Woolf

UCLA  
Nuclear Energy Laboratory  
405 Hilgard Avenue  
Los Angeles, CA 90024  
Attn: I. Catton

Westinghouse Corporation  
P. O. Box 355  
Pittsburgh, PA 15230  
Attn: N. Liparulo (3)  
J. Olhoeft  
V. Srinivas

Westinghouse Hanford Company  
P. O. Box 1970  
Richland, WA 99352  
Attn: G. R. Bloom (3)  
L. Muhlstein  
R. D. Peak

University of Wisconsin  
Nuclear Engineering Department  
1500 Johnson Drive  
Madison, WI 53706  
Attn: M. L. Corradini

Australian Atomic Energy Commission  
Private Mail Bag  
Sutherland, NSW 2232  
AUSTRALIA  
Attn: John W. Connolly

Director of Research, Science & Education  
CEC  
Rue De La Loi 200  
1049 Brussels  
BELGIUM  
Attn: B. Tolley

AEC, Ltd.  
Whiteshell Nuclear Research Establishment  
Pinawa, Manitoba, CANADA  
Attn: D. Liu (2)  
H. Tamm

McGill University  
315 Querbes  
Outremont, Quebec  
CANADA H2V 3W1  
Attn: John H. S. Lee (3)

CNEN NUCLIT  
Rome, ITALY  
Attn: A. Morici

Battelle Institut E. V.  
Am Roemerhof 35  
6000 Frankfurt am Main 90  
FEDERAL REPUBLIC OF GERMANY  
Attn: Dr. Werner Baukal

Gesellschaft fur Reakforsicherheit (GRS)  
Postfach 101650  
Glockengasse 2  
5000 Koeln 1  
FEDERAL REPUBLIC OF GERMANY  
Attn: Dr. M. V. Banaschik

Gesellschaft fur Reaktorsicherheit (GRS mbH)  
8046 Garching  
FEDERAL REPUBLIC OF GERMANY  
Attn: E. F. Hicken (2)  
H. L. Jahn

Institute fur Kernenergetik  
und Energiesysteme  
University of Stuttgart  
Stuttgart  
FEDERAL REPUBLIC OF GERMANY  
Attn: G. Froehlich (2)  
M. Buerger

Kernforschungszentrum Karlsruhe  
Postfach 3640  
75 Karlsruhe  
FEDERAL REPUBLIC OF GERMANY  
Attn: Dr. S. Hagen (3)  
Dr. J. P. Hosemann  
Dr. M. Reimann

Kraftwerk Union  
Hammerbacherstrasse 12 & 14  
Postfach 3220  
D-8520 Erlangen 2  
FEDERAL REPUBLIC OF GERMANY  
Attn: Dr. K. Hassman (2)

Technische Universitaet Muenchen  
D-8046 Garching  
FEDERAL REPUBLIC OF GERMANY  
Attn: Dr. H. Karwat

Swedish State Power Board  
El-Och Vaermeteknik  
SWEDEN  
Attn: Eric Ahlstroem

AERE Harwell  
Didcot  
Oxfordshire OX11 0RA  
UNITED KINGDOM  
Attn: J. Gittus, AETB (2)  
J. R. Matthews, TPD

Berkeley Nuclear Laboratory  
Berkeley GL 139PB  
Gloucestershire  
UNITED KINGDOM  
Attn: J. E. Antill

British Nuclear Fuels, Ltd.  
Building 396  
Springfield Works  
Salwick, Preston  
Lancs  
UNITED KINGDOM  
Attn: W. G. Cunliffe

National Nuclear Corp. Ltd.  
Cambridge Road  
Whetstone, Leicester, LE83LH  
UNITED KINGDOM  
Attn: R. May

Simon Engineering Laboratory  
University of Manchester  
M139PL,  
UNITED KINGDOM  
Attn: Prof. W. B. Hall

UFAEA Safety & Reliability Directorate  
Wigshaw Lane, Culcheth  
Warrington WA34NE  
Cheshire  
UNITED KINGDOM  
Attn: J. G. Collier  
S. F. Hall  
A. J. Wickett

(3)

Sandia

Distribution:

1131 W. B. Benedick  
1131 J. Fisk  
1512 J. C. Cummings  
1513 S. N. Kempka  
1513 A. C. Ratzel  
2512 V. M. Loyola (8)  
6400 A. W. Snyder  
6410 J. W. Hickman  
6411 V. L. Behr  
6411 S. E. Dingman  
6411 F. E. Haskin  
6411 A. L. Camp  
6420 J. V. Walker  
6420-A J. B. Rivard  
6422 D. A. Powers  
6423 K. Muramatsu  
6425 W. J. Camp  
6425 W. Frid  
6425 K. Schoenefeld  
6425 S. Unwin  
6427 M. Berman  
6427 K. P. Guay  
6427 J. T. Hitchcock  
6427 J. Kotas  
6427 M. S. Krein  
6427 B. W. Marshall, Jr.  
6427 L. S. Nelson  
6427 O. Seebold  
6427 M. P. Sherman  
6427 S. R. Tieszen  
6427 G. Valdez  
6427 M. J. Wester  
6427 C. C. Wong  
6440 D. A. Dahlgren  
6442 W. A. von Rieseemann  
6444 S. L. Thompson  
6445 E. H. Richards  
6449 K. D. Bergeron  
8024 M. A. Pound  
8513 W. J. McClean  
8523 P. M. Barr  
8523 K. D. Marx  
8523 B. R. Sanders  
3141 C. M. Ostrander (5)  
3151 W. G. Garner

NRC FORM 326 (2-84) NRCM 1102, 3201, 3202 <b>BIBLIOGRAPHIC DATA SHEET</b> SEE INSTRUCTIONS ON THE REVERSE		U.S. NUCLEAR REGULATORY COMMISSION 1 REPORT NUMBER (Assigned by T/DC add Vol. No. if any) NUREG/CR-3361 SAND83-1326	
2 TITLE AND SUBTITLE The Effect of Water Chemistry on the Rates of Hydrogen Generation from Galvanized Steel Corrosion at Post-LOCA Conditions		3 LEAVE BLANK	
5 AUTHOR(S) V. M. Loyola J. E. Womelsduff		4 DATE REPORT COMPLETED MONTH: November      YEAR: 1984	
7 PERFORMING ORGANIZATION NAME AND MAILING ADDRESS (Include Zip Code) Sandia National Laboratories P. O. Box 5800 Albuquerque, NM 87185		6 DATE REPORT ISSUED MONTH: December      YEAR: 1984	
10 SPONSORING ORGANIZATION NAME AND MAILING ADDRESS (Include Zip Code) Division of Accident Evaluation Containment Systems Research Branch Office of Nuclear Regulatory Research U. S. Nuclear Regulatory Commission Washington, D.C. 20555		8 PROJECT/TASK WORK UNIT NUMBER B&R No. 60191104	
12 SUPPLEMENTARY NOTES		9 FIN OR GRANT NUMBER NRC FIN No. A-1255	
13 ABSTRACT (200 words or less) <p>The rates of hydrogen generation are measured for the corrosion of galvanized steel in three different light water cooled reactor (LWR) water chemistries. The results were obtained over a temperature range of 100° to 175° C and indicate that in a boiling water reactor (BWR) water chemistry, the reaction is faster than in those of two pressurized water reactors (PWR's).</p> <p>A mechanism is proposed which would explain the observed results without requiring that the chemical additives come in direct contact with the corrodible unoxidized metal. Such a mechanism is required because electron microprobe analysis suggests that no chemical additives have diffused into the protective ZnO layer which forms on the unoxidized metal.</p> <p>Arrhenius parameters are calculated for the three chemistries, but some questions are raised about whether those parameters are associated with a diffusion process or with the actual hydrogen producing reaction.</p>		11a TYPE OF REPORT  b PERIOD COVERED (Indicate dates) 1/81 - 1/82	
14 DOCUMENT ANALYSIS - KEYWORDS-DESCRIPTORS Reactor Safety Post-LOCA Hydrogen Generation		15 AVAILABILITY STATEMENT	
6 IDENTIFIERS-OPEN ENDED TERMS Galvanized Steel Corrosion Hydrogen from Zinc		16 SECURITY CLASSIFICATION If the page: Unc. If the report: Unc.	
		17 NUMBER OF PAGES 35	
		18 PRICE	



120555078877 1 IANR3  
US NRC  
ADM-DIV OF TIDC  
POLICY & PUB MGT BR-PDR NUREG  
W-501  
WASHINGTON DC 20555